Enhanced Modelling of Split-Ring Resonators Couplings in Printed Circuits

Radovan Bojanic, Vojislav Milosevic, Branka Jokanovic, *Member, IEEE*, Francisco Medina-Mena, *Fellow, IEEE*, and Francisco Mesa, *Fellow, IEEE*

***Abstract*—An enhanced equivalent circuit approach for the magnetic/electric interaction of single split-ring resonators (SRRs) with printed lines is presented in this paper. A very simple and efficient lumped-element network is proposed to model the behavior of metamaterial-based printed lines over a wide frequency band. The same circuit topology can be used for the single- and two-mirrored SRRs loaded microstrip line. The corresponding circuit parameters are obtained from the multiconductor transmission line theory as well as from closed-form expressions that make use of just the resonance frequency and minimum of the reflection coefficient (which should be previously extracted from experiments or full-wave simulations). The comparison of our equivalent circuit results with measurements and full-wave simulations has shown a very good agreement in a considerably wider frequency band than other previously proposed simple equivalent circuits.**

***Index Terms*—Coupled transmission lines, equivalent circuit, metamaterial, microstrip line, split-ring resonator.**

I. Introduction

METAMATERIAL-BASED guiding structures have been intensively investigated in the past decade with the purpose of extending the operational capabilities of diverse passive and active components in antennas and microwave circuits [1]. A great deal of effort has specifically been devoted to the study of printed transmission lines loaded with parallel inductive or series capacitive elements [2]–[5]. Resonant-type metamaterial-based transmission lines (MMTLs) with double split ring resonators (SRRs) and complementary SRRs (CSRRs) have also been considered in the frame of the development of filters, sensors, and RFID tags [6]–[8], among other applications. One of the most interesting properties of the SRR is that the orientation and position of its gap with respect to the hosting transmission line has significant influence on the overall performance of the loaded transmission line. This topic has been previously studied by some of the authors of the present work [9] and has found potential application in designing reconfigurable delay lines and scanning antennas [10], [11].

Metamaterial transmission lines (like many other electromagnetic structures) can be reasonably modeled by lumped-element equivalent circuits. This approach is a useful tool for better understanding of the physics underlying the propagation phenomena in MMTLs. Also, a very important benefit of using the equivalent circuit is in independent parameter tuning and optimization of cascaded structures. These are still very time-consuming, despite the enormous progress in computational resources, especially if a great number of individual resonators is involved.

Equivalent circuits of MMTLs loaded with double SRRs with passband and stopband characteristics can be found, for instance, in [12] and [13], where coplanar waveguides (CPWs) were used as the background transmission lines. MMTLs based on microstrip lines mostly involve coupling with CSRRs [14] or fractal and multiple CSRRs [15] etched in the ground plane (right beneath the line) so that they are excited by the electric field perpendicular to the plane of the CSRR. The equivalent circuit of a double-SRR-loaded microstrip line with a vertical via was reported in [16] to explain its passband response. In all of these previous papers, the gaps of the double SRRs and CSRRs were oriented parallel to the transmission line. The cross-coupling effects resulting from the different orientations of double SRRs and CSRRs coupled to CPW and microstrip lines have been studied using the equivalent circuit approach in [17].

It should be noted that all of the examples mentioned above (except those in [16]) are double-sided structures, which are difficult to fabricate and assemble with other planar devices. This fact might limit their wide application in modern wireless systems, in which reduced size, cost, and simple integration are principal concerns. For these reasons, microstrip technology is possibly the best choice for integrating MMTLs and related components.

The present work studies square-shaped SRRs coupled to the microstrip line lying in the same plane. Gaps in the SRRs are either parallel (near to or far from the line) or perpendicular to the microstrip line, with the latter having cross-coupling effects. Both a single SRR placed at one side of the line and a pair of SRRs symmetrically/asymmetrically placed at both sides are

Manuscript received December 25, 2013; revised March 29, 2014; accepted June 12, 2014. Date of publication July 08, 2014; date of current version August 04, 2014. This work was supported by the Serbian Ministry of Education, Science and Technological Development through Projects TR-32024 and III-45016 and the project of bilateral cooperation between the Kingdom of Spain and the Republic of Serbia PRI-AIBSE-2011-1119. The work of F. Mesa and F. Medina-Mena was supported by the Spanish Ministry of Economy and Competitiveness under Projects TEC2010-16948 and CSD2008-00066. *(Corresponding author: Francisco Medina-Mena.)*

R. Bojanic, V. Milosevic, and B. Jokanovic are with the Institute of Physics, University of Belgrade, 11080 Belgrade, Serbia (e-mails: radovan@ipb.ac.rs; vojislav@ipb.ac.rs; brankaj@ipb.ac.rs).

F. Medina-Mena is with the Department of Electronics and Electromagnetism, Faculty of Physics, University of Seville, Seville, Spain (e-mail: medina@us.es).

F. Mesa is with the Department of Applied Physics 1, University of Seville, Seville, Spain (e-mail: mesa@us.es).

Color versions of one or more of the figures in this paper are available online at http://ieeexplore.ieee.org.

Digital Object Identifier 10.1109/TMTT.2014.2332302

considered. An equivalent circuit model is proposed and validated for an arbitrarily oriented single-SRR-loaded microstrip line. The topology of the circuit is slightly more complicated than other proposed approaches, in order to increase the bandwidth of the model. The new models make use of the same number of independent parameters as in previous simpler proposals, although they are now interconnected in a different way in order to capture the distributed nature of the original loaded transmission line more efficiently. The approximation to the distributed behavior could be further improved by adding more elements to the lumped-circuit representation, but this would increase the complexity of the model and the number of parameters to be determined.

The proposed unit cells exhibit a stopband response, and they can be used as basic components in the design of high-performance compact filters. The validity of the equivalent circuit models is confirmed by the S-parameters obtained from the measurements of laboratory samples and from full-wave electromagnetic simulations. The proposed circuit topology is also very suitable for the unit cells with passband response since via inductance can easily be taken into account without increasing the complexity of the model.

This paper is organized as follows. Section II presents the circuit parameter extraction using a coupled-lines model to obtain the parameters of the host line coupled to SRR. In Section III, the remaining parameters are calculated employing closed-form expressions that make use of the resonance frequencies and the reflection coefficient minimum obtained by full-wave simulations. Two types of equivalent circuit are considered for the loaded transmission line: with one and with two LC cells. The latter is found to provide a bandwidth two times wider. The equivalent circuit model is validated by comparison with full-wave simulations and measurements in Section IV. A very good agreement is found in a wide frequency range, not only for structures with a single unit cell but also for structures with a cascade of SRR unit cells.

II. Circuit Parameters Extraction Using a Coupled-Lines Model

In order to obtain the equivalent circuit models of microstrip lines loaded with arbitrarily oriented SRRs, having their gaps parallel or perpendicular to the line (both near and far from the line), two configurations are examined: 1) a single SRR at one side of the microstrip line and 2) two SRRs at both sides of the line. The equivalent circuit of an arbitrarily oriented single-SRR-loaded microstrip line has not been considered so far, with the exception of the modeling of the mutual coupling between SRRs themselves reported in [18].

The SRR-loaded microstrip line with the gap parallel (and close) to the line is shown in Fig. 1, together with the relevant dimensions. A similar structure, but involving double SRRs, has been studied in [16], where the equivalent circuit shown in Fig. 2(a) is proposed. The transmission line is represented by a single Π-cell. In this paper, we propose the enhanced model shown in Fig. 2(b), where the line is represented by two Π-cells. We will demonstrate that this circuit, which has the same number of independent parameters as the previous one, allows much better matching with full-wave simulations and measurements.

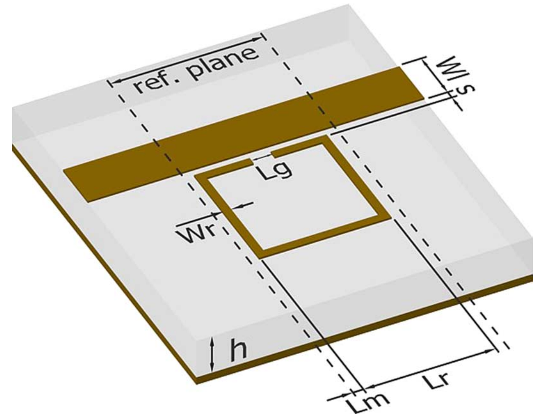

Fig. 1. Layout of the microstrip line loaded with SRR with the relevant dimensions: $h = 1.27$ mm, $L_r = 3$ mm, $L_m = 0.25$ mm, $L_g = 0.5$ mm, $W_r = 0.2$ mm, $W_l = 1.2$ mm, $S = 0.1$ mm. The metalization thickness is $t = 17\ \mu$m, and the dielectric permittivity $\varepsilon_r = 10.2$.

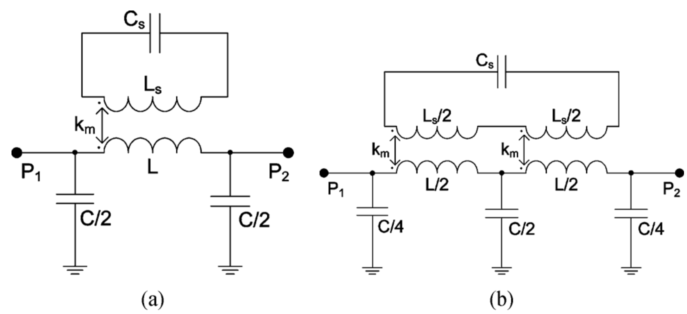

Fig. 2. Equivalent circuit of the microstrip line loaded with SRR consisting of (a) one and (b) two Π-cells.

To extract the parameters L and C of the transmission line (Fig. 2), taking into account the coupling between the line and the nearest SRR arm, the system is modeled as a section of the multiconductor transmission line. LINPAR software [19] is employed for the numerical evaluation of the quasistatic line parameters. LINPAR provides the per unit length (p.u.l.) inductance and capacitance matrices from which the required parameters of the finite-length coupled-line sections are obtained.

According to the coupling geometry between the SRRs and the transmission line, the structures under study have been divided into five groups, as shown in Table I. Depending on the orientation of the SRR, the microstrip line is coupled with the whole SRR side or by two parts of the side separated by the gap.

In Table I, three types of marked sections can be distinguished: the isolated section and the coupled section with one or two SRR arms. The parameters of each section have been calculated using diagonal elements of the p.u.l. inductance and capacitance matrices. The resulting parameters L and C of the microstrip line (given in the second column of Table I) are obtained by summing the parameters of individual sections. It can be seen that the transmission-line inductance L is very similar for all configurations, but the capacitance C varies much more (15%) depending on the configuration, i.e., on the coupling between the SRR and the line. The SRR

TABLE I
CONFIGURATIONS OF SRRS COUPLED WITH THE MICROSTRIP LINE AND EXTRACTED PARAMETERS. COUPLING HAS BEEN TAKEN INTO ACCOUNT ONLY BETWEEN THE SECTIONS MARKED BY HATCHING. REFERENCE PLANES ARE DENOTED BY DOTTED LINES

(a)	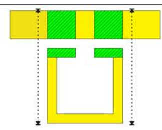	$L = 1.51\,\mathrm{nH}$ $C = 0.72\,\mathrm{pF}$ $L_s = 7.97\,\mathrm{nH}$
(b)	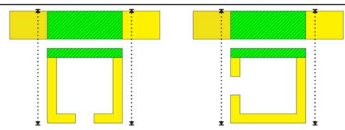	$L = 1.51\,\mathrm{nH}$ $C = 0.74\,\mathrm{pF}$ $L_s = 7.92\,\mathrm{nH}$
(c)	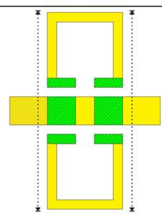	$L = 1.5\,\mathrm{nH}$ $C = 0.82\,\mathrm{pF}$ $L_s = 7.97\,\mathrm{nH}$
(d)	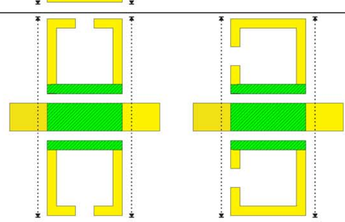	$L = 1.5\,\mathrm{nH}$ $C = 0.86\,\mathrm{pF}$ $L_s = 7.92\,\mathrm{nH}$
(e)	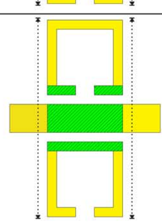	$L = 1.5\,\mathrm{nH}$ $C = 0.84\,\mathrm{pF}$ $L_{s1} = 7.97\,\mathrm{nH}$ $L_{s2} = 7.92\,\mathrm{nH}$

inductance L_S consists of two parts: 1) from the section that is coupled with the transmission line, which is calculated using the corresponding diagonal element of the inductance matrix, and 2) from an isolated transmission line with length equal to the remaining uncoupled part of the SRR length. Values of L_S given in Table I are slightly different due to the fact that coupled-line sections have a somewhat lower p.u.l. inductance than isolated ones. Hereinafter, we adopt the same values for the inductances, $L = 1.5$ nH and $L_S = 8$ nH, for all of the considered configurations.

III. CIRCUIT PARAMETERS EXTRACTION USING FULL-WAVE ANALYSIS

It has been found that different configurations of SRR loaded microstrip line can be modeled by the same circuit topology, but with different values of the circuit parameters. According to the circuit topology, all considered configurations can be divided into three groups: 1) SRRs with gaps parallel to the line; 2) two SRRs with parallel gaps near and far from the line; and 3) SRRs with gaps perpendicular to the line. For each topology, closed-form expressions for the resonance frequency and the minimum reflection frequency can be obtained. Those expressions are then used to determine the remaining circuit parameters (magnetic coupling coefficient k_m and SRR capacitance C_s), based on the

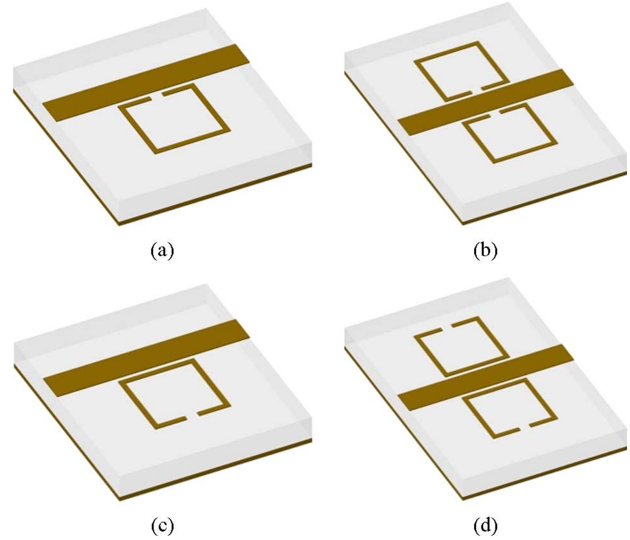

Fig. 3. Microstrip line loaded with SRRs with gaps parallel to the line. (a) One SRR with gap near the line. (b) Two SRRs with gaps near the line. (c) One SRR with gap far from the line. (d) Two SRRs with gaps far from the line. These configurations can be modeled by the equivalent circuits in Fig. 2.

frequencies computed through full-wave simulations. The only parameter that has to be fitted is the electric coupling coefficient k_e; i.e., coupling capacitance $C_m = k_e\sqrt{CC_s}$, in the case of SRR with perpendicular gaps (this coefficient is introduced in Section III-C).

A. Microstrip Line Loaded With SRRs With Gaps Parallel to the Line

Microstrip lines loaded with SRRs with gaps parallel to the line are shown in Fig. 3. The equivalent circuit parameters L, C, and L_S are given in Table I for each configuration in Fig. 3 (they depend on their geometry and material characteristics). The remaining parameters C_S and k_m are determined using the S-parameters obtained by full-wave simulation. It should be noted that, in the frequency range of interest, the full-wave simulation only shows one S_{11} minimum that is located below the resonance frequency while both equivalent circuits exhibit two S_{11} minima: one below and the other above the resonance. The presence of this upper spurious parasitic S_{11} minimum certainly reduces the bandwidth, where it is possible to obtain a good matching between simulations and equivalent circuit analysis. However, the equivalent circuit with two Π-cells [Fig. 2(b)] moves that minimum to higher frequencies with respect to the one cell model, as will be discussed later.

The capacitance C_S is obtained from the SRR resonance frequency $f_r = \omega_r/2\pi$ as follows:

$$f_r = \frac{1}{2\pi\sqrt{L_S C_S}}. \quad (1)$$

1) S_{11} Minimum of the Equivalent Circuit Model Below the Resonance: The magnetic coupling coefficient k_m is determined by the frequency of the first minimum of S_{11}, $f_{\min} = \omega_{\min}/2\pi$, for the equivalent circuits in Fig. 2. In order to simplify calculations, we can apply Bartlett's bisection theorem [20]. The coupling coefficient k_m is then obtained as a function of $f_{\min}$, the resonance frequency f_r, and the line parameters L and C as follows:

$$k_m^2 = \left(1 - \frac{\omega_r^2}{\omega_{\min}^2}\right)(1 - a_{1,2}) \tag{2}$$

where a_1 corresponds to the circuit with one cell [Fig. 2(a)] and a_2 is for the two cells circuit [Fig. 2(b)]. These coefficients are given by

$$a_1 = \left[\frac{L}{C}Y_0^2 + 2b\right]^{-1} \tag{3}$$

$$a_2 = \left[\frac{L}{C}Y_0^2\left(1 - \frac{b}{2-b}\right) + b\right]^{-1} \tag{4}$$

where Y_0 is the characteristic admittance of the microstrip line (20 mS in our case), and

$$b = \left(\frac{\omega_{\min}}{\omega_0}\right)^2; \quad \omega_0^2 = \frac{8}{LC}.$$

Full-wave simulations and measurements for all of the structures in Fig. 3 show that the S_{11} minimum appears before the resonance of the SRR f_r, making the first parenthesis in (2) negative. In order to obtain a real value of the coupling coefficient k_m (which allows for the matching between the frequencies of first minima of S_{11} obtained by full-wave simulation and those obtained by equivalent circuit analysis), it is necessary for the right-hand side of that equation to be positive, which requires $a_{1,2} > 1$.

In Fig. 4(a) and (b), we show a comparison of the a-coefficients calculated for one and two cells, respectively, for the SRR coupled to the 50-Ω microstrip line [Fig. 3(a)] on different substrates. From the position of the S_{11} minimum (corresponding markers), it can be seen that the condition $a > 1$ is not satisfied in any case in Fig. 4(a). On the other hand, that condition is fulfilled for all cases in Fig. 4(b). Also, the substrate with the highest permittivity (Rogers RO3010) exhibits the lowest upper frequency of the bandwidth in which k_m has a real value (3.51 GHz for one cell and 7.02 GHz for two cells). It should be noted that the a-coefficient is not a function of SRR parameters, but only of the S_{11} minimum frequency and the parameters of the background transmission line.

Fig. 4(a) and (b) clearly shows that the important advantage of the enhanced modeling of SRR loaded transmission line, compared with the one Π-cell equivalent circuit, is that it provides a bandwidth two times wider in which k_m has real values.

If a grounding via was present, a passband response would be obtained, and the S_{11} minimum would appear above the transmission zero in a full-wave simulation. In such case, a good agreement can be achieved with the equivalent circuit where the line is represented by only one cell [16]. In that case, our proposed equivalent circuit would become very similar to the

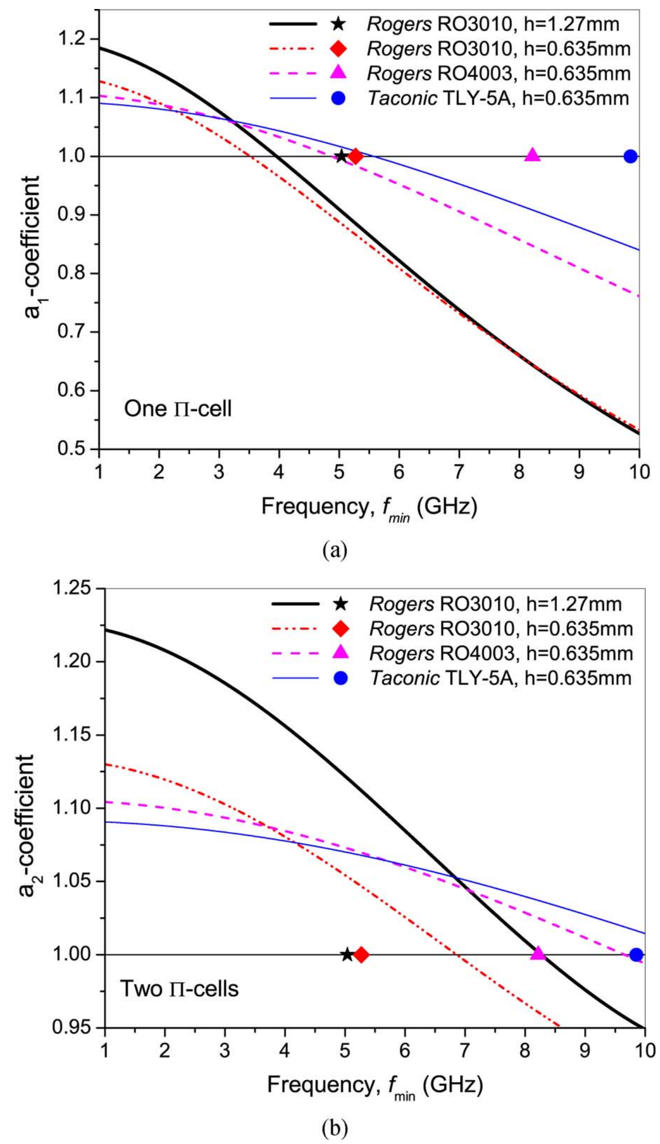

Fig. 4. Comparison of the a-coefficient for the equivalent circuit with (a) one and (b) two Π-cells for the case in Fig. 3(a). Horizontal black lines indicate the value of 1 on the vertical axis, and markers denote the frequency of S_{11} minimum for the corresponding substrates. For real values of the coupling coefficient k_m, the coefficients $a_{1,2}$ should be greater than 1.

improved model reported in [13], in which one cell is modified to allow for positioning of a centered via inductance.

2) S_{11} Minimum of the Equivalent Circuit Model Above the Resonance: Both equivalent circuit models in Fig. 2 exhibit a second S_{11} minimum above the resonance frequency of the SRR, which does not appear in the full-wave simulations or measurements. This spurious effect is a consequence of approximating a distributed circuit by lumped elements. In order to improve the bandwidth in which the equivalent circuit can be used, it is necessary to push that parasitic minimum towards high frequencies. This has been done by using the equivalent circuit with two Π-cells.

To clarify this, we start from the condition of perfect matching (minimum of S_{11}) for the symmetric circuit (following Bartlett's theorem): $Y_{\text{in,even}}Y_{\text{in,odd}} = Y_0^2$, where even and odd admittances are calculated by placing an open/short

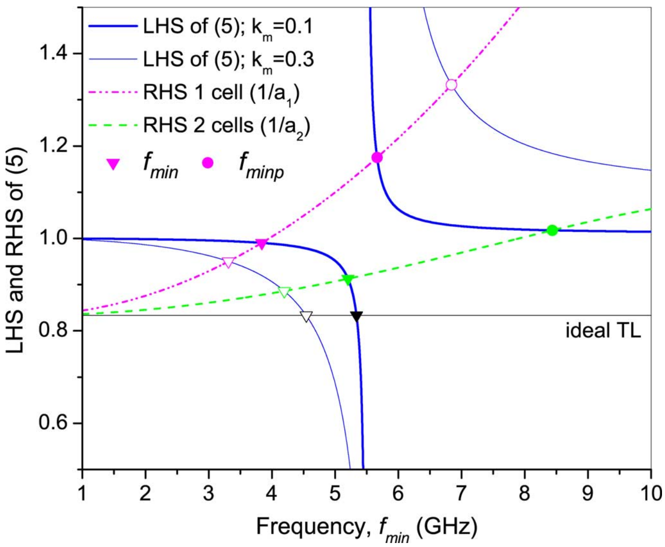

Fig. 5. Plotted LHS (solid curves) and RHS (dashed curves) of (5). Crossings indicate S_{11} minima for corresponding cases.

TABLE II
EXTRACTED PARAMETERS FOR THE CONFIGURATIONS IN FIG. 3

Configurations	f_r(GHz)	$f_{\min}$(GHz)	C(pF)	C_S(pF)	k_m
Fig. 3(a)	5.47	5.04	0.72	0.107	0.14
Fig. 3(b)	5.48	5.14	0.82	0.106	0.167
Fig. 3(c)	6.19	4.84	0.74	0.084	0.28
Fig. 3(d)	6.14	4.72	0.86	0.088	0.41

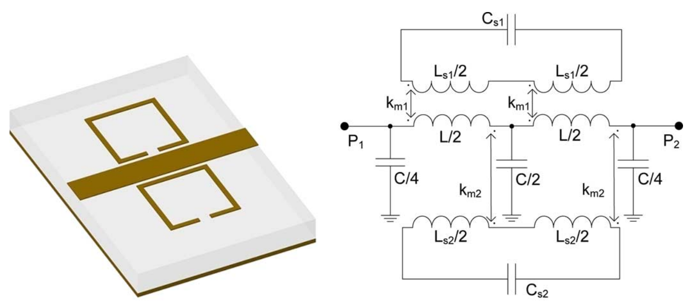

(a) (b)

Fig. 6. (a) Microstrip line loaded with two SRRs with parallel gaps near and far from the line. (b) Corresponding equivalent circuit.

termination at the symmetry plane. After some rearrangements, the equivalent condition can be reformulated as

$$\frac{\omega_r^2 - \omega_{\min}^2}{\omega_r^2 - (1-k_m^2)\omega_{\min}^2} = a_{1,2}^{-1} \tag{5}$$

where values of $a_{1,2}$ correspond to (3) and (4) for one and two cells, respectively. At low frequencies, a_2 can be approximated as $a_2^{-1} \approx (L/C)Y_0^2 + (b/2)$. Comparing this expression with (3), it is observed that the coefficient accompanying the term b is four times smaller. Since b is proportional to the square of the frequency [see (4)], this implies that a_2 varies two times slower with frequency then a_1, thus showing a frequency behavior closer to that expected for an ideal transmission line (which should give a constant value of the a-coefficient).

In Fig. 5 the left-hand side (LHS) and right-hand side (RHS) of (5) are plotted for one and two cells and for two different coupling coefficients [the transmission line parameters correspond to the case in Fig. 3(a)]. The crossings of the corresponding curves for LHS and RHS indicate solutions of (5) and, therefore, frequencies of S_{11} minima. Crossings below the SRR resonance are marked with triangles, and they represent the real minima of the S_{11} parameter, while the crossings above the resonance, marked with circles, are the parasitic minima $f_{\min\mathrm{p}}$, absent in full-wave simulation. The LHS of this equation does not depend on the number of cells but only on the coupling coefficient k_m and resonance f_r (solid curves). By increasing the coupling strength, this curve "widens" (compare thick and thin curves) so that it is possible to adjust the frequencies of both S_{11} minima in a given range. Moreover, the RHS depends only on the transmission line parameters L and C (which are basically determined by the choice of the substrate and characteristic impedance), and it has a completely different slope for the simple and the enhanced equivalent circuits. It can readily be observed from the figure that the RHS corresponding to the enhanced equivalent circuit is much more favorable in regards to the parasitic minimum, $f_{\min\mathrm{p}}$, of S_{11}, as it appears at much higher frequencies than those corresponding to the conventional circuit. In particular, for small values of the coupling coefficient ($k_m \sim 0.1$), the second S_{11} minimum appears right above the one-cell circuit resonance, therefore severely reducing its usable bandwidth, as opposed to the case of the enhanced equivalent circuit.

3) Extracted Equivalent Circuit Parameters: Extracted parameters for the two-cell equivalent circuit [Fig. 2(b)] are given in Table II for all configurations in Fig. 3. The difference in C_S is due to different resonance frequencies, according to (1). The magnetic coupling coefficient k_m is very different and is much greater for the structures without gaps in the arm near the line, where the coupling is the most pronounced.

B. Microstrip Line Loaded With Two SRRs With Parallel Gaps Near and Far From the Line

A microstrip line loaded with two SRRs with parallel gaps near and far from the line [Fig. 6(a)] has a more complex equivalent circuit [Fig. 6(b)] than in the previous case. It is a superposition of two equivalent circuits given in Fig. 2(b), because the SRRs have two different magnetic couplings and resonance frequencies.

The values of the extracted parameters $C_{s1} = 0.105$ pF and $C_{s2} = 0.081$ pF have been determined from the resonance frequencies f_{r1} and f_{r2}, computed with a full-wave simulator.

The magnetic coupling coefficients $k_{m1,2}$ are determined by applying Bartlett's theorem to the circuit in Fig. 6(b), in a similar way as for the circuit in Fig. 2(b). To obtain $k_{m1,2}$, the following system of two equations has to be solved (since there are two S_{11} minima, $f_{\min 1,2}$):

$$\frac{\omega_{\min1}^2}{\omega_{r1}^2-\omega_{\min1}^2}k_{m1}^2 + \frac{\omega_{\min1}^2}{\omega_{r2}^2-\omega_{\min1}^2}k_{m2}^2 = a_2^{(1)} - 1$$
$$\frac{\omega_{\min2}^2}{\omega_{r1}^2-\omega_{\min2}^2}k_{m1}^2 + \frac{\omega_{\min2}^2}{\omega_{r2}^2-\omega_{\min2}^2}k_{m2}^2 = a_2^{(2)} - 1 \tag{6}$$

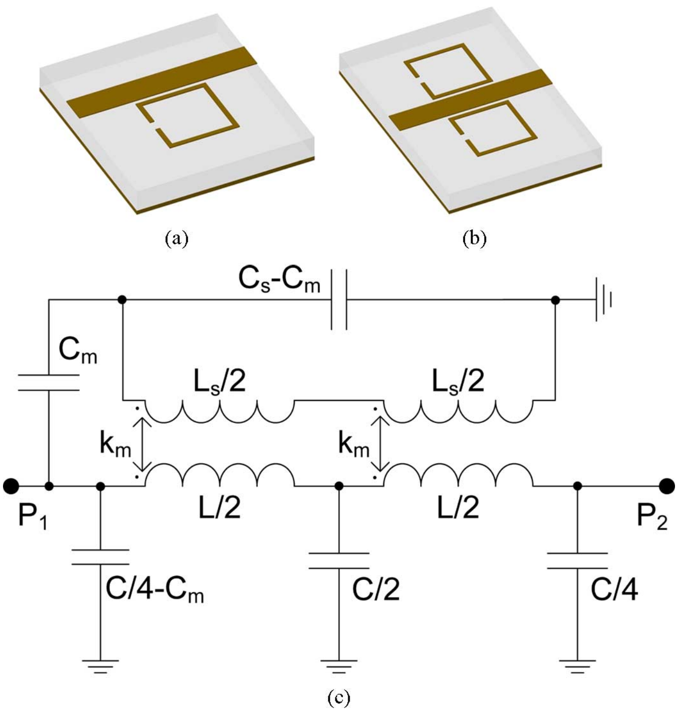

Fig. 7. Microstrip line loaded with SRRs with gaps perpendicular to the line. (a) Single SRR. (b) Two SRRs mirrored with respect to the line, which can be modeled by (c) the same equivalent circuit.

where $a_2^{(1),(2)}$ are calculated according to (4). Finally, it is obtained $k_{m1} = 0.14$ and $k_{m2} = 0.26$.

For the equivalent circuit with one Π-cell, the system (6) will remain the same, except that a_2 is replaced by a_1, calculated according to (3). In this case, the first equation in (6) corresponds to the first minimum of S_{11} below the resonances. Thus the coefficients on the LHS will be positive, and the RHS turns out to be negative, which is impossible to solve. Consequently, it is impossible to overlap the first minimum with full-wave simulations and measurements. The second minimum, however, falls between two resonances; therefore, one of the coefficients at LHS in the second equation in (6) is negative, so it is possible to overlap this minimum. For this case, it is found the following relation between coupling coefficients:

$$k_{m1}^2 = \left(\omega_{\min 2}^2 - \omega_{r1}^2\right)\left(\frac{k_{m2}^2}{\omega_{r2}^2 - \omega_{\min 2}^2} - \frac{a_1^{(2)} - 1}{\omega_{\min 2}^2}\right). \quad (7)$$

When solving (7), which has multiple solutions, it should be taken into account that k_{m2} (corresponding to the SRR with the gap far from the line) should be greater than k_{m1}.

C. Microstrip Line Loaded With SRRs With Gaps Perpendicular to the Line

The SRRs depicted in Fig. 7 differ from the previous configurations as they have been rotated 90°, which means that the structure is no longer symmetric with respect to the microstrip line. In this case, the electric field of the line is parallel to the gap, which causes additional electric coupling, included in the equivalent circuit model shown in Fig. 7(c).

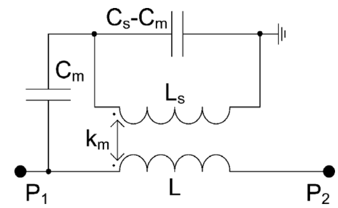

Fig. 8. Simplified circuit for the calculation of the resonance frequency.

A microstrip line loaded with one SRR with the gap perpendicular to the line [Fig. 7(a)] has the same equivalent circuit as two mirrored SRRs symmetrically placed at both sides of the line [Fig. 7(b)], but with different values of circuit elements.

The corresponding equivalent circuit parameters L, C and L_S are given in Table I for each configuration in Fig. 7. The magnetic coupling coefficient k_m for the structures in Fig. 7(a) and (b) are approximated by the values obtained for the corresponding SRRs with gaps parallel and far from the microstrip line [Fig. 3(c) and (d), respectively], since they have very similar surface current distributions. The remaining parameters, C_S and C_m, are determined using the resonance frequency (C_S is determined as function of C_m, which is derived through a fitting procedure with full-wave simulation).

To calculate the approximate resonance frequency (i.e., minimum of S_{21}), we use the equivalent circuit shown in Fig. 8, in which the shunt capacitors are removed with respect to the circuit in Fig. 7(c). This makes the circuit analysis significantly easier while the resonance is hardly affected.

After writing the system of equations according to Kirchhoff's laws, the following matrix relation between currents and voltages at ports 1 and 2 is obtained:

$$\begin{bmatrix} j\omega\left(\frac{1-L_S}{L_m}\right) & 1 \\ \frac{j}{\omega L_m}(1-\omega^2 L_S C_S) + j\omega C_m & 0 \end{bmatrix}\begin{bmatrix} V_1 \\ I_1 \end{bmatrix} = \begin{bmatrix} -\frac{j\omega C_m L_S}{L_m} & 1-\omega^2 L_m C_m\left(\frac{1}{k_m^2}-1\right) \\ \frac{j}{\omega L_m}(1-\omega^2 L_S C_S) & \frac{L}{L_m}(1-\omega^2 L_S C_S(1-k_m^2)) \end{bmatrix} \cdot \begin{bmatrix} V_2 \\ I_2 \end{bmatrix}. \quad (8)$$

The condition for the resonance can be expressed as having a nontrivial solution on the LHS when $V_2, I_2 = 0$ (i.e., the RHS should be equal to zero), which is only satisfied when the determinant of the matrix on LHS is equal to zero as follows:

$$\frac{j}{\omega L_m}(1-\omega^2 L_S C_S) + j\omega C_m = \frac{j}{\omega L_m}(1-\omega^2 L_S C_S + \omega^2 L_m C_m) = 0 \quad (9)$$

which gives the following resonance frequency:

$$f_r = \frac{1}{2\pi\sqrt{L_S C_S - L_m C_m}} \quad (10)$$

TABLE III
EXTRACTED PARAMETERS FOR THE CONFIGURATIONS IN FIG. 7

Configurations	f_r(GHz)	C(pF)	C_S(pF)	k_m	C_m(pF)
Fig. 7(a)	5.8	**0.74**	0.102	**0.29**	**0.055**
Fig. 7(b)	5.86	**0.86**	0.108	**0.42**	**0.08**

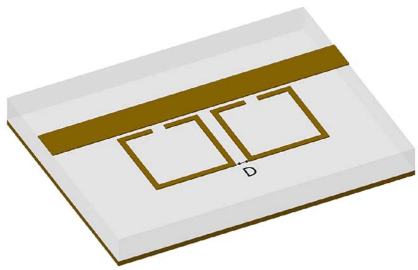

(a)

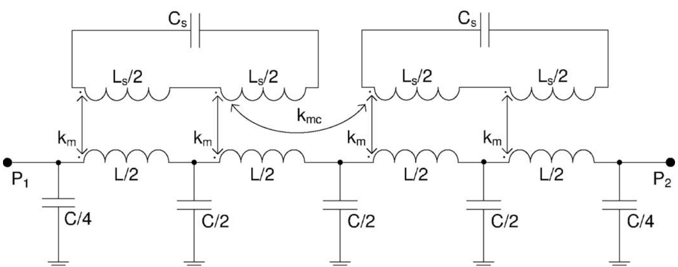

(b)

Fig. 9. (a) Cascaded SRRs. (b) Corresponding equivalent circuit.

with $L_m = k_m\sqrt{LL_S}$. It can be proved that, due to reciprocity ($S_{12} = S_{21}$), the LHS and RHS matrices of (8) have equal determinants, but it is simpler to consider the one on the LHS.

The extracted values of the equivalent circuit elements (Table III) are obtained after a slight optimization of C_s, C_m and k_m parameters, required because of the simplified circuit analysis. It can be seen that the values of L, C_s and L_s are very similar for both structures but C, C_m and k_m are different. The differences in C_m and k_m are a consequence of the stronger coupling in the case with two SRRs.

D. Cascaded Structures

The unit cells discussed above can be cascaded in order to design filters with improved bandwidth, as shown in Fig. 9(a) for SRRs with the gaps parallel and close to the line. This structure is modeled by the equivalent circuit shown in Fig. 9(b), with the previously extracted parameters, and with an additional inter-resonator coupling that depends on the distance D between the SRRs. The coupling coefficient k_{mc} is determined from full-wave simulation of two resonators, and can be used for modeling an arbitrary number of SRRs as long as nonadjacent resonator coupling can be neglected. The obtained coupling coefficients k_{mc} for different inter-resonator distances are shown in Table IV.

IV. VALIDATION OF THE MODEL AND RESULTS

To validate the proposed equivalent circuit models and the extracted circuit parameters, the magnitudes and phases of the

TABLE IV
EXTRACTED INTER-RESONATOR COUPLING COEFFICIENTS, k_{mc}

D (mm)	0.1	0.2	0.3	0.4	0.5
k_{mc}	0.155	0.102	0.078	0.052	0.03

(a)

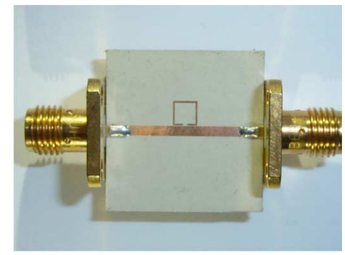

(b)

Fig. 10. (a) Fabricated custom designed LRL calibration set for the measurement of S-parameters at reference planes. (b) Microstrip line loaded with SRR with parallel gap close to the line.

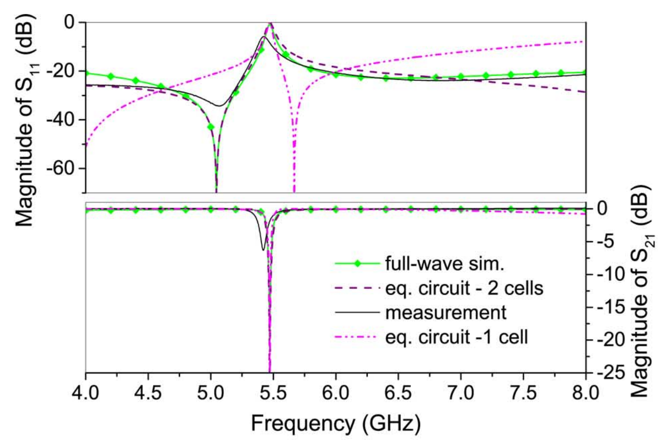

(a)

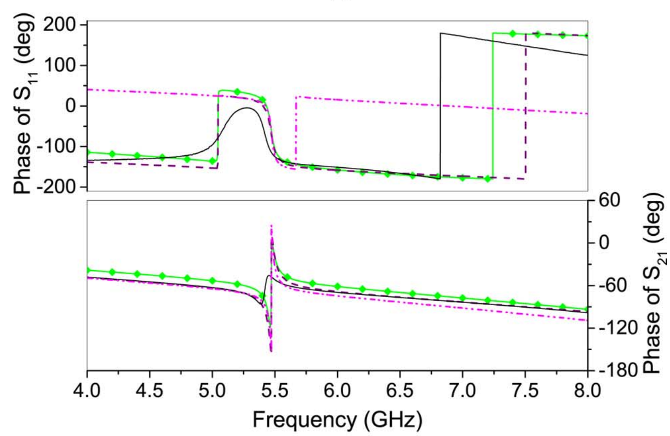

(b)

Fig. 11. Comparison of magnitudes (a) and phases (b) of S-parameters obtained by measurements, full-wave simulations, and equivalent circuit analysis with one and two Π-cells for the configuration in Fig. 3(a).

S-parameters obtained by measurements, full-wave simulations and equivalent circuit analysis are compared. Full-wave simulations are performed using lossless materials, since the equivalent circuit models do not include any losses. Nevertheless, some losses are still present both in full-wave simulations and measurements due to radiation. Certainly, the measured

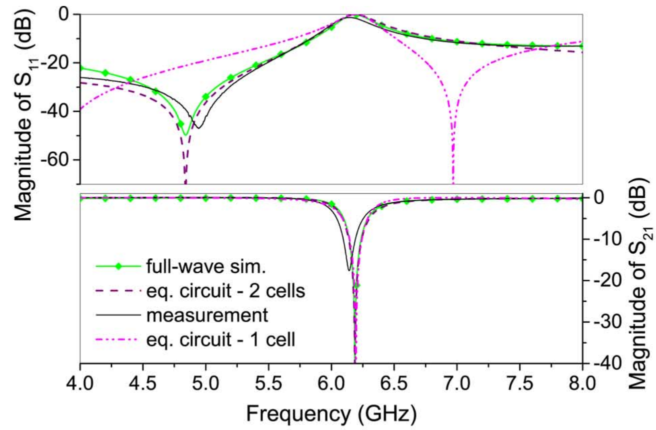

(a)

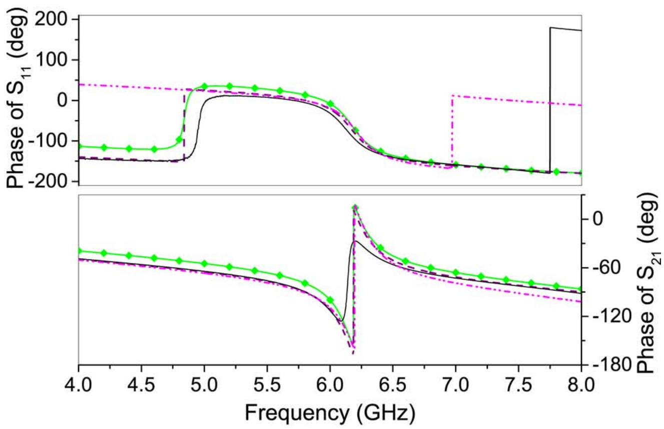

(b)

Fig. 12. Comparison of (a) magnitudes and (b) phases of S-parameters obtained by measurements, full-wave simulations, and equivalent circuit analysis with one and two Π-cells for the configuration in Fig. 3(c).

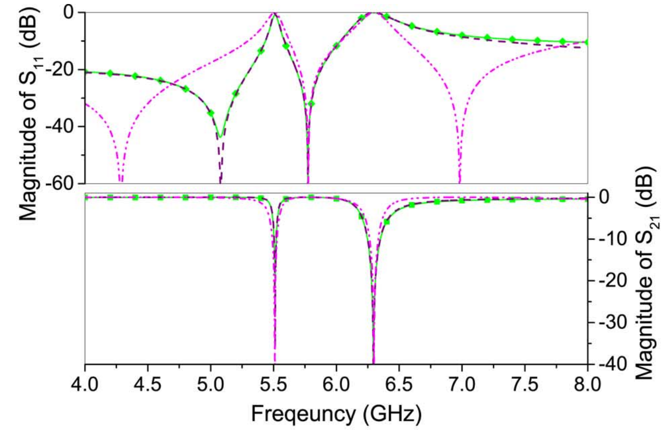

(a)

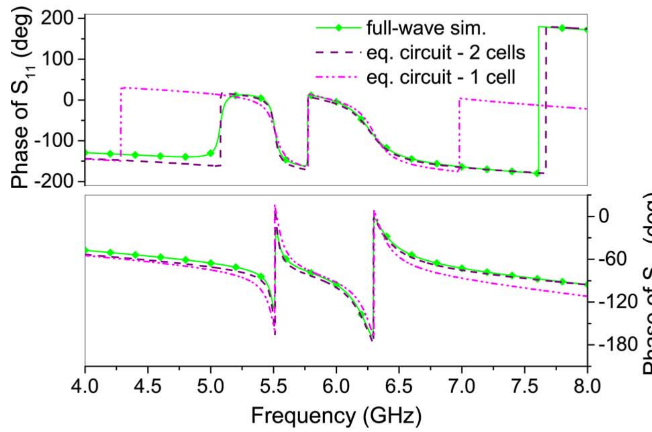

(b)

Fig. 13. Comparison of (a) magnitudes and (b) phases of S-parameters obtained by full-wave simulations and equivalent circuit analysis with one and two Π-cells for the configuration in Fig. 6(a).

results include the actual losses in the metal and dielectric. All structures are simulated using WIPL-D software [21], and results are de-embedded at the reference planes marked in Fig. 1. Measured S-parameters are also de-embedded at the reference planes using the LRL (Line-Reflect-Line) calibration set shown in Fig. 10(a), and the Anritsu ME7838A VNA. A fabricated prototype of the microstrip line loaded with a single SRR with gap parallel (and close) to the line is shown in Fig. 10(b).

A. Microstrip Line Loaded With SRRs With Gaps Parallel to the Line

The results obtained by measurement, full-wave simulation, and equivalent circuit analysis using two Π-cells [Fig. 2(b)] for structures in Fig. 3(a) and (c) are shown in Figs. 11 and 12, respectively. They are in good agreement in the whole frequency range from 4 to 8 GHz. Small discrepancies in magnitude between the equivalent circuit model and measurements in Fig. 11 are found at the end of the swept band and are attributed to the presence of the parasitic S_{11} minimum. The frequency of this minimum is around 8.8 GHz due to relatively weak coupling (see Fig. 5). In contrast to that, the results obtained with the one-cell equivalent circuit model [Fig. 2(a)] show a big discrepancy with the full-wave simulations and measurements for any value of k_m. Actually, this simplified model only works properly at the resonance frequency and in a very small region around it. The first minimum of S_{11} occurs at a far lower frequency than the measured one, and it is not possible to overlap them for any real value of k_m, in accordance with (3). The coupling coefficients for the equivalent circuits with one cell are obtained by a fitting procedure and their values are $k_m = 0.1$ in Fig. 11 and $k_m = 0.23$ in Fig. 12, for SRR with the gap far from the line.

B. Microstrip Line Loaded With Two SRRs With Parallel Gaps Near and Far From the Line

Comparison between the full-wave simulation and the equivalent circuit analysis with one and two cells is given in Fig. 13. For the case of the equivalent circuit with two cells we can see that almost perfect agreement is obtained in magnitude and phase in the whole frequency range from 4 to 8 GHz.

For the one-cell equivalent circuit, the good matching is obtained only around the second minimum with the coupling coefficient $k_{m1} = 0.16$ and $k_{m2} = 0.18$, which is not expected since the coupling structures are very different (with and without the gap). It can be seen that around the second resonance there is discrepancy not only in S_{11} but also in S_{21} characteristics, since it

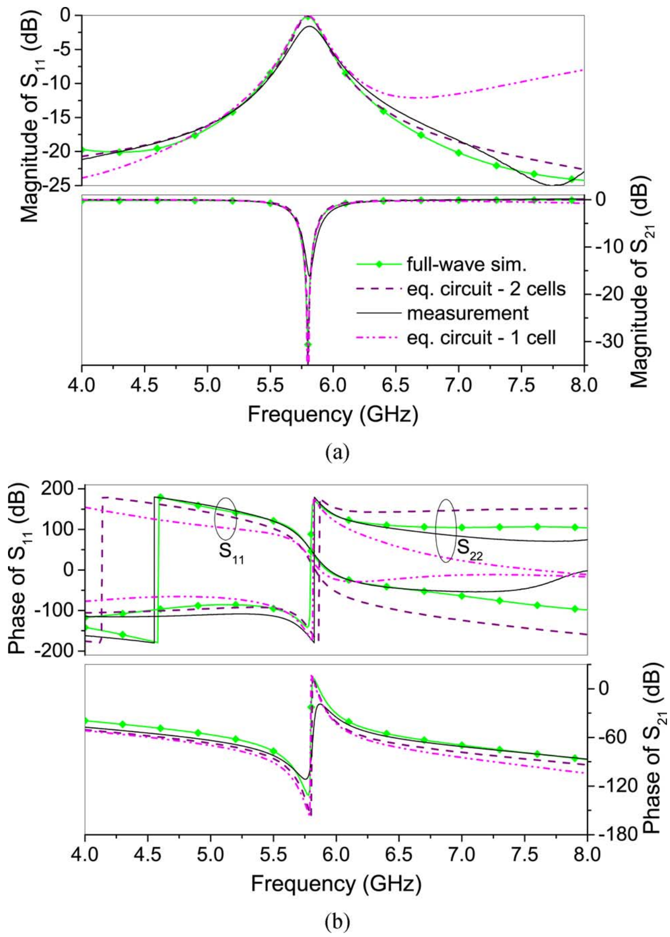

Fig. 14. Comparison of magnitudes (a) and phases (b) of S-parameters obtained by measurements, full-wave simulations, and equivalent circuit analysis with one and two Π-cells for the configuration in Fig. 7(a).

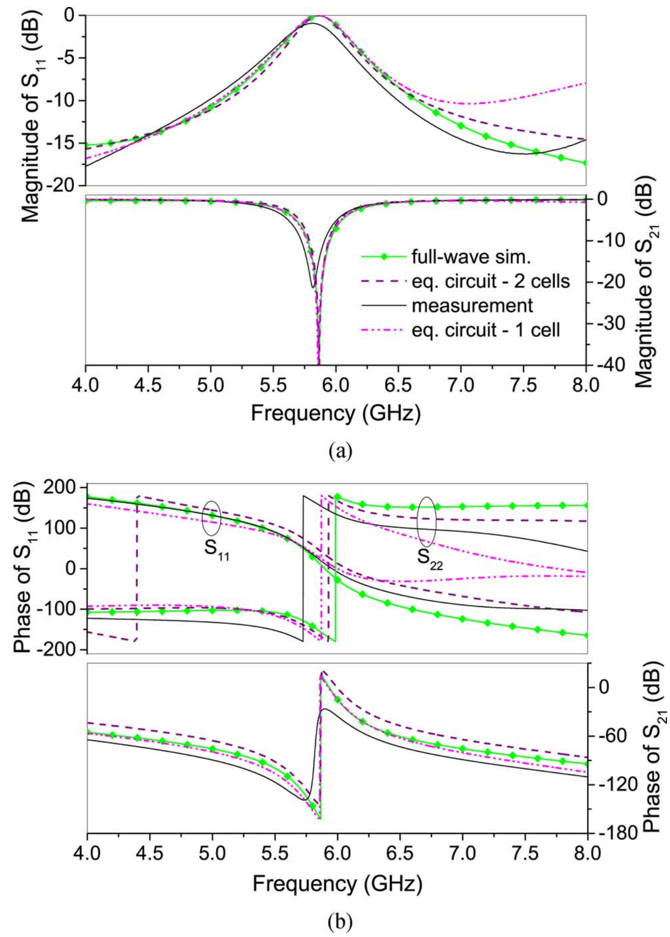

Fig. 15. Comparison of (a) magnitudes and (b) phases of S-parameters obtained by full-wave simulations and equivalent circuit analysis with one and two Π-cells for the configuration in Fig. 7(b).

is not feasible to move the third minimum to a higher frequency. Also, the first minimum in the S_{11} characteristic is not possible to match at all with one-cell equivalent circuit, as we had already predicted in Section III-A.

C. Microstrip Line Loaded With SRRs With Gaps Perpendicular to the Line

To show the advantages of the proposed enhanced equivalent circuit [Fig. 7(c)] with respect to the one-cell model for the SRR with gap perpendicular to the line [Fig. 7(a)], we compared in Fig. 14 magnitudes and phases of S-parameters obtained by measurements, full-wave simulations, and equivalent circuit models with one and two Π-cells. Once again, the results for the two-cell equivalent circuit model are in very good agreement with full-wave simulation and measurements in the whole frequency range from 4 to 8 GHz. It is important to mention that SRRs with the gap perpendicular to the line do not exhibit the first minimum of reflection below the resonance as the SRR with the gap parallel to the line. Although the structure is asymmetric, only the magnitude of the reflection S_{11} is shown (the difference with S_{22} only concerns the phase). The one-cell equivalent circuit seems to perform now much better than in the case with the parallel gap, but the proposed two-cell model still works better in a wider frequency band. The extracted parameters of one-cell model are $k_m = 0.28$, $C_m = 0.062$ pF.

The results of full-wave simulations and equivalent circuit model analysis with one and two Π-cells for the configuration in Fig. 7(b) are shown in Fig. 15. The results from the equivalent circuit model with two cells are in very good agreement with full-wave simulations. The one-cell model fits the full-wave simulations in a wider frequency range than for the corresponding single SRR and matching is good up to 7.5 GHz. The extracted circuit parameters for one-cell model are $k_m = 0.39$ and $C_m = 0.095$ pF.

D. Cascaded SRRs With Gaps Parallel to the Line

The results of full-wave simulations and equivalent circuit model analysis with one and two Π-cells for the configuration in Fig. 9, for inter-resonator distance $D = 0.5$ mm, are shown in Fig. 16. A very good agreement is found in the whole frequency band of interest, both in magnitude and phase of the S-parameters, between the two Π-cell model and the full-wave simulations. In contrast to that, the one Π-cell model is unable to match the reflection except in a very narrow range around resonance.

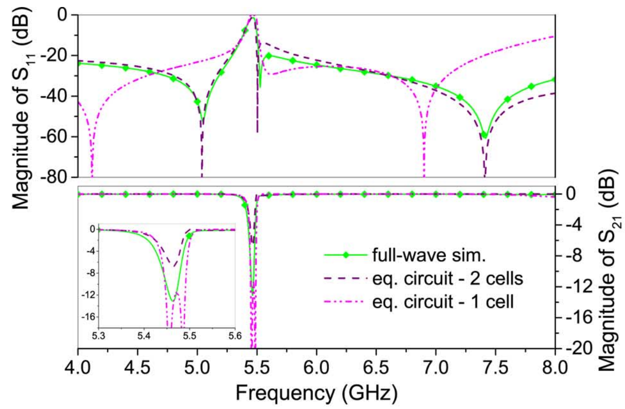

(a)

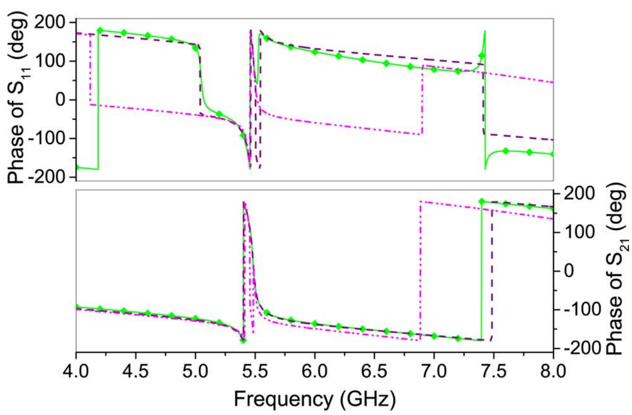

(b)

Fig. 16. Comparison of (a) magnitudes and (b) phases of S-parameters obtained by full-wave simulations and equivalent circuit analysis with one and two Π-cells for the configuration in Fig. 9, for distance $D = 0.5$ mm.

The values of magnetic coupling coefficients are obtained by fitting, and they are $k_m = 0.1$ and $k_{mc} = 0.015$.

V. Conclusion

Enhanced equivalent circuit models of microstrip lines loaded with single split-ring resonators have been proposed. Different orientations, not previously considered, of the SRR with respect to the line are analyzed: with the parallel gap near and far from the line, and with the gap perpendicular to the line. The printed line can be loaded with a single SRR at one side, or with two SRRs symmetrically/asymmetrically placed with respect to the line. This type of structures exhibits stop band response, but the proposed equivalent circuit model can easily be extended to structures with passband response by simply adding inductance between two Π-cells.

The single SRR (at one side of the line) and the two mirrored (with respect to the line) SRRs have the same equivalent circuit, although different circuit parameters. These are calculated using the multiconductor transmission-line model (L, C, L_s), while other necessary parameters (C_s and k_m) are obtained using closed-form expressions that relate them to the resonance frequency and minimum of reflection obtained by full-wave simulations. The only parameter to be optimized is the electric coupling present in the case of SRRs with gap perpendicular to the line.

The main advantage of the proposed two-cell circuit model is that it provides a twice wider bandwidth in which it is possible to match the minimum of reflection obtained by full-wave simulations. This is achieved without increasing the number of circuit parameters with respect to the one-cell circuit model. Also, the enhanced equivalent circuit approximates the distributed nature of the background transmission line in a better way, and moves the parasitic minimum above the SRR resonance to significantly higher frequencies, compared to the one-cell model. Therefore, the achieved good matching bandwidth is considerably increased.

A number of samples have been fabricated and measured to validate the parameters extraction procedure. Very good agreement between measured S-parameters, full-wave simulations, and the proposed two-cell equivalent circuit has been demonstrated over a wide frequency range, both in magnitude and phase. In contrast, the conventional one-cell model has been shown to work only in a narrow frequency band. The proposed model is easily extendible to cascaded structures, as it has been exemplified with two unit cells with different inter-resonator spacing. The cascaded model is validated by comparison with full-wave simulations, and very good agreement is observed.

Acknowledgment

The authors would like to thank the Institute IMTEL, Belgrade, for the fabrication of the prototypes and WIPL-D Belgrade for the use of software licenses.

References

[1] A. Lay, T. Itoh, and C. Caloz, “Composite right/left-handed transmission line metamaterials,” *IEEE Microw. Mag.*, vol. 5, no. 3, pp. 34–50, Mar. 2004.

[2] A. K. Iyer and G. V. Eleftheriades, “Negative refractive index metamaterials supporting 2-D waves,” in *IEEE MTT-S Int. Microw. Symp. Dig.*, 2002, vol. 2, pp. 412–415.

[3] C. Caloz and T. Itoh, “Application of the transmission line theory of left-handed (LH) materials to the realization of a microstrip LH transmission line,” in *Proc. IEEE-AP-S USNC/URSI Nat. Radio Sci. Meeting*, 2002, vol. 2, pp. 412–415.

[4] A. A. Oliner, “A periodic-structure negative-refractive-index medium without resonant elements,” in *IEEE-AP-S USNC/URSI Nat. Radio Sci. Meeting URSI Dig.*, 2002, vol. 2, p. 41.

[5] C. Caloz and T. Itoh*, Electromagnetic Metamaterials: Transmission Line Theory and Microwave Applications*. New York, NY, USA: Wiley-IEEE Press, 2006.

[6] J. García-García, J. Bonache, I. Gil, F. Martín, M. C. Velazquez-Ahumada, and J. Martel, “Miniaturized microstrip and CPW filters using coupled metamaterial resonators,” *IEEE Trans. Microw. Theory Techn.*, vol. 54, no. 6, pp. 2628–2635, Jun. 2006.

[7] J. Naqui, M. Durán-Sindreu, and F. Martín, “Alignment and position sensors based on split ring resonators,” *Sensors*, vol. 12, no. 9, pp. 11790–11797, Sep. 2012.

[8] F. J. Herraiz-Martínez, F. Paredes, G. Zamora, F. Martín, and J. Bonache, “Printed magnetoinductive-wave (MIW) delay lines for chipless RFID applications,” *IEEE Trans. Antennas Propag.*, vol. 60, no. 11, pp. 5075–5082, Nov. 2012.

[9] V. Milosevic, B. Jokanovic, and B. Kolundzija, “Microwave stereometamaterials and parameter extraction,” in *Metamaterials’2010: Proc. 4th Int. Congr. Adv. Electromagn. Materials Microw. Opt.*, Karlsruhe, Germany, Sep. 13–16, 2010, pp. 474–477.

[10] R. Bojanic, B. Jokanovic, and V. Milosevic, “Multiband delay lines with reconfigurable split-ring resonators,” in *Proc. 10th Int. Conf. Telecommun. Modern Satellite, Cable and Broadcasting Services*, Nis, Serbia, Oct. 5–8, 2011, pp. 31–34.

[11] N. Boskovic, B. Jokanovic, and A. Nesic, "Compact frequency scanning antenna array with SRR phase shifters," in *Proc. 11th Int. Conf. Telecommun. Modern Satellite, Cable and Broadcasting Services*, Nis, Serbia, Oct. 16–19, 2013, pp. 437–439.

[12] J. D. Baena, J. Bonache, F. Martin, R. Marques, F. Falcone, T. Lepetegi, M. Laso, J. Garcia-Garcia, I. Gil, M. F. Portillo, and M. Sorolla, "Equivalent-circuit models for split-ring resonators and complementary split-ring resonators coupled to planar transmission lines," *IEEE Trans. Microw. Theory Techn.*, vol. 53, no. 4, pp. 1451–1461, Apr. 2005.

[13] F. Aznar, M. Gil, J. Bonache, L. Jelinek, J. D. Baena, R. Marqués, and F. Martín, "Characterization of miniaturized metamaterial resonators coupled to planar transmission lines through parameter extraction," *J. Appl. Phys.*, vol. 104, Dec. 2008, Art. ID 114501.

[14] F. Falcone, T. Lepetegi, J. D. Baena, R. Marqués, F. Martín, and M. Sorolla, "Effective negative-epsilon stopband microstrip lines based on complementary split ring resonators," *IEEE Microw. Wireless Compon. Lett.*, vol. 14, pp. 280–282, Jun. 2004.

[15] V. Crnojevic-Bengin, V. Radonic, and B. Jokanovic, "Fractal geometries of complementary split-ring resonators," *IEEE Trans. Microw. Theory Techn.*, vol. 56, no. 10, pp. 2312–2321, Oct. 2008.

[16] I. Gil, J. Bonache, J. García-García, F. Falcone, and F. Martín, "Metamaterials in microstrip technology for filter applications," in *Proc. APS-URSI*, Washington, DC, USA, Jul. 2005, vol. 1a, pp. 668–671.

[17] J. Naqui, M. Durán-Sindreu, and F. Martín, "Modeling Split-Ring Resonator (SRR) and Complementary Split-Ring Resonator (CSRR) loaded transmission lines exhibiting cross-polarization effects," *IEEE Antennas Wireless Propag. Lett.*, vol. 12, no. 3, pp. 178–181, Mar. 2013.

[18] J. S. Hong and M. J. Lancaster, "Couplings of microstrip square open-loop resonators for cross-coupled planar microwave filters," *IEEE Trans. Microw. Theory Techn.*, vol. 44, no. 12, pp. 2099–2109, Dec. 1996.

[19] A. R. Djordjevic, M. B. Bazdar, T. K. Sarkar, and R. F. Harrington, *LINPAR for Windows: Matrix Parameters for Multiconductor Transmission Lines, Software and User's Manual*. Norwood, MA, USA: Artech House, 1995.

[20] E. A. Guillemin, *Synthesis of Passive Networks: Theory and Methods Appropriate to the Realization and Approximation Problems*. Melbourne, FL, USA: Krieger, 1977, p. 207.

[21] *"Software and User's Manual,"* WIPL-D d.o.o, Belgrade, Serbia, 2010.

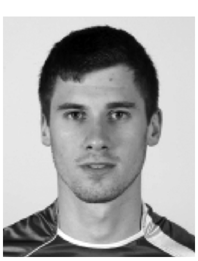

Radovan Bojanic was born in Knin, Croatia, in 1986. He received the Dipl.Ing. and M.Sc. degrees in electrical engineering from the University of Belgrade, Belgrade, Serbia, in 2009 and 2012, respectively, where he is currently working toward the Ph.D. degree.

Since 2010, he has been with the Institute of Physics, Belgrade, Serbia, as a Research Assistant with the Photonic Center, where he has been involved in modelling and simulation of microwave circuits.

Mr. Bojanic was the recipient of the Aleksandar Marincic Award from the Serbian National Society for Microwave Techniques, Technologies and Systems for the Best Paper in 2013.

Vojislav Milosevic was born in Belgrade, Serbia, on April 5, 1986. He received the Dipl. Ing. and M.Sc. degrees in electrical engineering from the University of Belgrade, Belgrade, Serbia, in 2009 and 2012, respectively, where he is currently working toward the Ph.D. degree.

In 2010, he became a Research Assistant with the Photonic Center, Institute of Physics, Belgrade, Serbia. His current research interests include electromagnetic metamaterials and homogenization theory.

Mr. Milosevic was the recipient of the Aleksandar Marincic Award from the Serbian National Society for Microwave Techniques, Technologies and Systems for the Best Paper in 2013.

Branka Jokanovic (M'89) received the Dipl. Ing., M.Sc., and Ph.D. degrees in electrical engineering from the University of Belgrade, Belgrade, Serbia, in 1977, 1988, and 1999, respectively.

She is currently a Research Professor with the Institute of Physics, University of Belgrade, Belgrade, Serbia. Before she joined the Photonic Center, Institute of Physics, she was the Head of the Microwave Department, Institute IMTEL, Belgrade. Her current research interests include modelling, simulation and characterization of microwave and photonic metamaterials for wireless communications and sensors.

Dr. Jokanovic was one of the founders of the Yugoslav IEEE Microwave Theory and Techniques Society (MTT-S) Chapter and its chairperson from 1989 to 2000. She also founded the Yugoslav Association for Microwave Techniques and Technology in 1994 and initiated the Yugoslav MTT journal *Microwave Review* for which she was the editor for six years (1994–2000). She received the IMTEL Institute Award for Scientific Contribution in 1996, the 2000 IEEE Third Millennium Award, the YU MTT Distinguished Service Award in 2005, and Aleksandar Marincic Award in 2013. She is a corresponding member of the Serbian Academy of Engineering Sciences.

Francisco Medina-Mena (M'90–SM'01–F'10) was born in Puerto Real, Cádiz, Spain, in November 1960. He received the Licenciado and Ph.D. degrees from the University of Seville, Seville, Spain, in 1983 and 1987, respectively, both in physics.

He is currently a Professor of electromagnetism with the Department of Electronics and Electromagnetism, University of Seville, Seville, Spain, and Head of the Microwaves Group. His research interest includes analytical and numerical methods for planar structures, anisotropic materials, and artificial media modelling. He has coauthored approximately 130 book chapters and journal papers on those topics as well as more than 250 conference contributions.

Prof. Medina-Mena acts as a reviewer for more than 40 IEEE, IEE, AIP and IoP journals among others and has been member of the TPCs of a number of local and international conferences on his topics.

Francisco Mesa (M'93–SM'11–F'14) was born in Cádiz, Spain. He received the Licenciado and Ph.D. degrees in physics from the University of Seville, Seville, Spain, in 1989 and 1991, respectively.

He is currently a Professor with the Department of Applied Physics, University of Seville, Seville, Spain. His research interests focus on electromagnetic propagation/radiation in planar structures.

Prof. Mesa is currently serving as an associate editor of the IEEE TRANSACTIONS ON MICROWAVE THEORY AND TECHNIQUES.